JACC: CARDIOVASCULAR IMAGING
VOL. ■, NO. ■, 2017

ISSN 1936-878X/$36.00
PUBLISHED BY ELSEVIER
http://dx.doi.org/10.1016/j.jcmg.2017.04.021

Scar Characterization to Predict Life-Threatening Arrhythmic Events and Sudden Cardiac Death in Patients With Cardiac Resynchronization Therapy

The GAUDI-CRT Study

Juan Acosta, MD,[a,b] Juan Fernández-Armenta, MD, PhD,[a,b] Roger Borràs, MSc,[a,b] Ignasi Anguera, MD, PhD,[c] Felipe Bisbal, MD, PhD,[b,d] Julio Martí-Almor, MD, PhD,[e] Jose M. Tolosana, MD, PhD,[a,b] Diego Penela, MD, PhD,[a,b] David Andreu, MSc, PhD,[a,b] David Soto-Iglesias, MSc,[a,b] Reinder Evertz, MD,[a,b] María Matiello, MD,[f] Concepción Alonso, MD, PhD,[g] Roger Villuendas, MD,[b,d] Teresa M. de Caralt, MD, PhD,[h] Rosario J. Perea, MD, PhD,[h] Jose T. Ortiz, MD, PhD,[a,b] Xavier Bosch, MD, PhD,[a,b] Luis Serra, PhD,[i] Xavier Planes, MsC,[i] Andreas Greiser, PhD,[j] Okan Ekinci, MD, MBA,[k,l] Luis Lasalvia, MD, MIB,[m] Lluis Mont, MD, PhD,[a,b] Antonio Berruezo, MD, PhD[a,b]

ABSTRACT

OBJECTIVES The aim of this study was to analyze whether scar characterization could improve the risk stratification for life-threatening ventricular arrhythmias and sudden cardiac death (SCD).

BACKGROUND Among patients with a cardiac resynchronization therapy (CRT) indication, appropriate defibrillator (CRT-D) therapy rates are low.

METHODS Primary prevention patients with a class I indication for CRT were prospectively enrolled and assigned to CRT-D or CRT pacemaker according to physician's criteria. Pre-procedure contrast-enhanced cardiac magnetic resonance was obtained and analyzed to identify scar presence or absence, quantify the amount of core and border zone (BZ), and depict BZ distribution. The presence, mass, and characteristics of BZ channels in the scar were recorded. The primary endpoint was appropriate defibrillator therapy or SCD.

RESULTS 217 patients (39.6% ischemic) were included. During a median follow-up of 35.5 months (12 to 62 months), the primary endpoint occurred in 25 patients (11.5%) and did not occur in patients without myocardial scar. Among patients with scar ($n = 125$, 57.6%), those with implantable cardioverter-defibrillator (ICD) therapies or SCD exhibited greater scar mass (38.7 ± 34.2 g vs. 17.9 ± 17.2 g; $p < 0.001$), scar heterogeneity (BZ mass/scar mass ratio) (49.5 ± 13.0 vs. 40.1 ± 21.7; $p = 0.044$), and BZ channel mass (3.6 ± 3.0 g vs. 1.8 ± 3.4 g; $p = 0.018$). BZ mass (hazard ratio: 1.06 [95% confidence interval: 1.04 to 1.08]; $p < 0.001$) and BZ channel mass (hazard ratio: 1.21 [95% confidence interval: 1.10 to 1.32]; $p < 0.001$) were the strongest predictors of the primary endpoint. An algorithm based on scar mass and the absence of BZ channels identified 148 patients (68.2%) without ICD therapy/SCD during follow-up with a 100% negative predictive value.

CONCLUSIONS The presence, extension, heterogeneity, and qualitative distribution of BZ tissue of myocardial scar independently predict appropriate ICD therapies and SCD in CRT patients. (J Am Coll Cardiol Img 2017;■:■–■)
© 2017 by the American College of Cardiology Foundation.

From the [a]Arrhythmia Section, Cardiology Department, Thorax Institute, Hospital Clínic and IDIBAPS (Institut d'Investigació Agustí Pi i Sunyer), University of Barcelona, Barcelona, Catalonia, Spain; [b]CIBERCV, Instituto de Salud Carlos III, Madrid, Spain; [c]Cardiology Department, Heart Disease Institute, Bellvitge Biomedical Research Institute IDIBELL, Bellvitge Hospital, University of Barcelona, Spain; [d]Heart Institute (iCor), University Hospital Germans Trias i Pujol, Barcelona, Spain; [e]Electrophysiology Unit, Cardiovascular Division, Department of Medicine, Hospital del Mar, Universitat Autònoma de Barcelona, Barcelona, Spain; [f]Arrhythmia Section, Cardiology Department, Catalonia General Hospital, Barcelona, Spain; [g]Arrhythmia Unit, Cardiology Department, Hospital de la Sta. Creu i St. Pau, Barcelona, Spain; [h]Radiology Department,

ABBREVIATIONS AND ACRONYMS

3D = 3-dimensional

ATP = antitachycardia pacing

AUC = area under the curve

BZ = border zone

CI = confidence interval

ce-CMR = contrast-enhanced cardiac magnetic resonance

CRT = cardiac resynchronization therapy

CRT-D = cardiac resynchronization therapy with defibrillator

CRT-P = cardiac resynchronization therapy with pacemaker

HR = hazard ratio

ICD = implantable cardioverter-defibrillator

LV = left ventricle/ventricular

LVEF = left ventricular ejection fraction

MPSI = maximum pixel signal intensity

NYHA = New York Heart Association

PP = primary prevention

SCD = sudden cardiac death

VA = ventricular arrhythmia

VT = ventricular tachycardia

Cardiac resynchronization therapy (CRT), with or without an implantable defibrillator (CRT-D), reduces mortality and improves cardiac function in symptomatic chronic heart failure patients with depressed left ventricular ejection fraction (LVEF) and prolonged QRS duration (1,2). The survival benefit of CRT-D over a CRT pacemaker (CRT-P) is not well established. Current guidelines recommend CRT-D or CRT-P implantation in primary prevention (PP) patients with the same level of evidence (3). Most PP patients with CRT indication receive a CRT-D, although only a minority of these individuals (15% to 18%) require implantable cardioverter-defibrillator (ICD) therapies during follow-up (1,4). Therefore, better risk-stratification tools are required in order to identify those CRT patients at high risk of life-threatening ventricular arrhythmias (VAs) that could benefit from CRT-D implantation.

Myocardial scar provides the substrate for VAs. Contrast-enhanced cardiac magnetic resonance (ce-CMR) allows an accurate identification and quantification of myocardial scar tissue, and enables the differentiation between the scar core and border zone (BZ) (5–7). Although several studies have shown the utility of scar characterization for risk stratification of VAs in ICD patients (5,6), its role in CRT patients is less well defined. The issue of scar characterization for risk stratification of VAs in CRT patients becomes especially interesting given that CRT response has been associated with a reduction of the risk of VA (2); however, it remains unknown whether this is influenced by the presence/absence of scar and its characteristics. We conducted a multicenter study with long-term follow-up to test the hypothesis that scar characterization by ce-CMR could improve the risk stratification of life-threatening VAs and sudden cardiac death (SCD) in PP patients with a CRT indication.

METHODS

STUDY DESIGN AND POPULATION. This was a prospective, observational multicenter study. Consecutive PP patients with heart failure, dilated cardiomyopathy, LVEF <35%, and wide QRS (>120 ms) who were referred for CRT were prospectively enrolled at 6 centers in Barcelona (Spain). The type of CRT (CRT-D vs. CRT-P) was decided according to physician's criteria before study inclusion. ce-CMR was performed before device implantation to assess left ventricular (LV) function and to identify and characterize scar tissue. Patients with contraindications to ce-CMR or those in whom ce-CMR could not be performed due to logistical reasons were excluded. Patients with diagnosis of noncompaction cardiomyopathy were also excluded due to its intrinsic arrhythmogenic capabilities and the impossibility of appropriate segmentation on noncompacted areas. After implantation, 2-zone detection was programmed in all patients: fast ventricular tachycardia (VT) (170 to 220 beats/min) and ventricular fibrillation (>220 beats/min). Supraventricular tachycardia discrimination algorithms were programmed for the VT zone. In all CRT-D patients, shock (plus antitachycardia pacing [ATP] during charging when possible) was programmed in the ventricular fibrillation zone. Programming or not ICD therapies in the fast VT zone was left to the discretion of the treating physician. The fast-VT zone therapy was ATP at 91% and 81% of tachycardia cycle length with 10-ms scan followed by shocks.

All patients provided written informed consent to participate. The local ethics committee approved this study.

CONTRAST-ENHANCED CMR. The ce-CMR study was performed either using a 1.5-T (n = 144, 66.4%) or a 3-T (n = 73, 33.6%) clinical scanner. See the Online Appendix for details.

Hospital Clinic, University of Barcelona, Barcelona, Catalonia, Spain; [i]Galgo Medical, SL, Barcelona, Spain; [j]Siemens Healthcare GmbH, Erlangen, Germany; [k]Siemens Healthineers, Chief Medical Office, Erlangen, Germany; [l]University College Dublin, School of Medicine, Dublin, Ireland; and [m]Siemens Medical Solutions, Global Clinical Marketing, Siemens Healthineers, New York, New York. This study has been supported by Siemens Healthcare and performed in collaboration with the Clinical Competence Center Cardiology, Erlangen, Germany. This work was also supported in part by the project PI14/00759, integrated in the Plan Nacional de I+D+I, and cofinanced by the ISCIII-Subdirección General de Evaluación and the Fondo Europeo de Desarrollo Regional (FEDER), and by Sociedad Española de Cardiología (Proyecto de Invetigación Sección de Arritmias y Electrofisiología). Dr. Serra and Mr. Planes are stockholders and employees of Galgo Medical SL. Dr. Greiser is an employee of Siemens Healthcare. Dr. Ekinci is an employee of Siemens Healthineers. Dr. Lasalvia is a stockholder and employee of Siemens Healthcare. Dr. Berruezo is a stockholder in Galgo Medical SL; and has received financial support from Siemens Healthcare. All other authors have reported that they have no relationships relevant to the contents of this paper to disclose.

Manuscript received December 20, 2016; revised manuscript received April 13, 2017, accepted April 27, 2017.

FIGURE 1 **Image Processing**

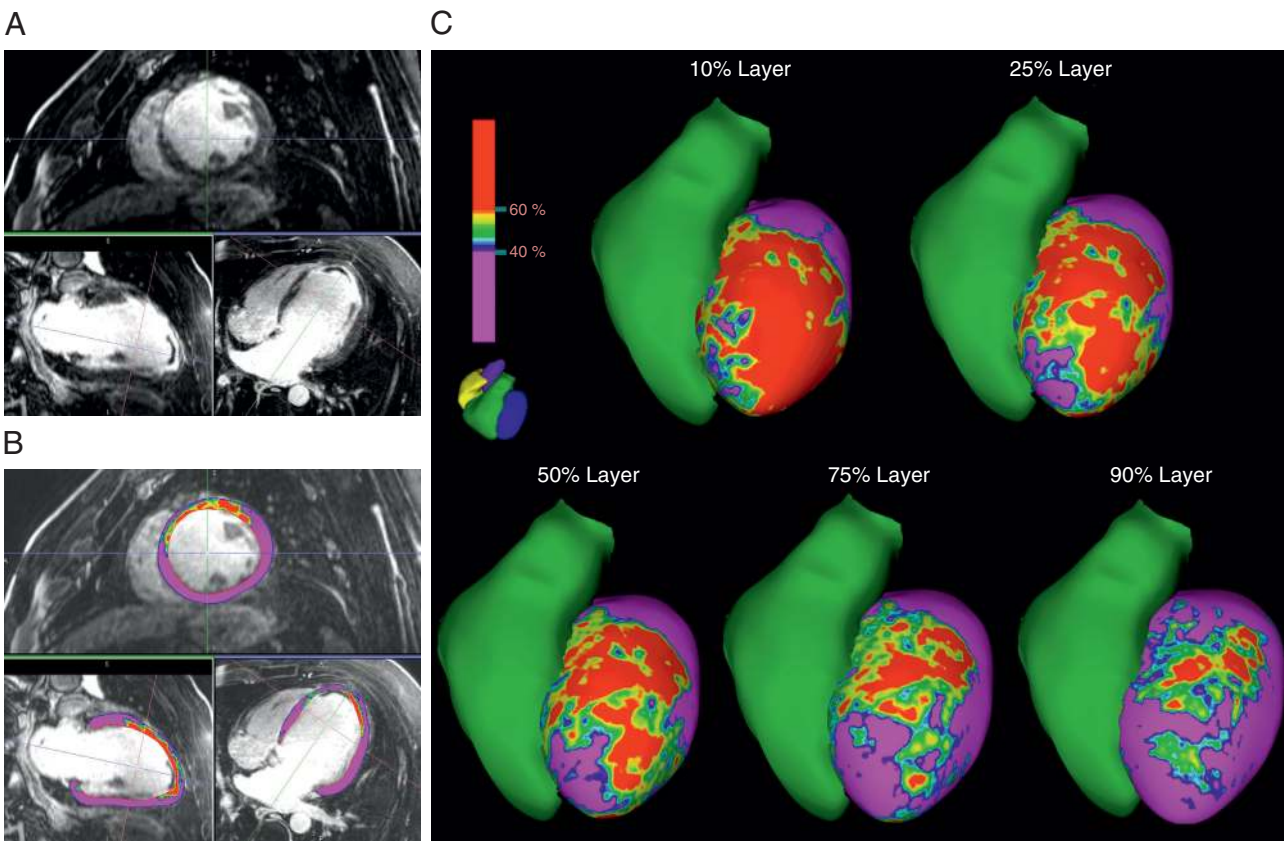

(A) Short-axis view, 2-chamber view, and 4-chamber view of contrast-enhanced magnetic resonance showing a transmural scar in the anterior wall of the left ventricle. **(B)** Concentric layers from the endocardium to epicardium were created and were color-coded according to signal intensity (normal myocardium is in **purple**, border zone in **green**, and core in **red**). **(C)** 3-Dimensional color-coded signal intensity maps in 5 transmural shells were obtained representing the scar, shape, and distribution of the scar tissue across the wall thickness.

Myocardial scar quantification and characterization. All ce-CMR images were analyzed with the segmentation program TCTK (Tissue Characterization Tool Kit, Barcelona, Spain) in a central core lab. An experienced observer, blinded to the clinical data, delineated the myocardial fibrosis region in all short-axis slices. The myocardial-fibrosis tissue was divided into core and BZ using an algorithm based on maximum pixel signal intensity (MPSI). The core was defined as a region with signal intensity >60% of MPSI in the scar area, whereas BZ was established as the region with signal intensity <60% and >40% of MPSI, as previously described (8). Total core and BZ mass were obtained by multiplying the number of the voxels of each region by voxel mass, as previously described (9).

Identification of BZ channels. Identification of BZ channels was performed in a central core lab. Using an investigational software tool (ADAS, Galgo Medical SL, Barcelona, Spain), a 3-dimensional (3D) model of the LV showing endocardial and epicardial borders was obtained using a semiautomated segmentation algorithm. Once the model was obtained, 5 concentric surface layers from the endocardium to epicardium were created (10%, 25%, 50%, 75%, and 90% of the LV wall thickness).

Using the same thresholds described previously to differentiate the scar core from the BZ and the BZ from the healthy tissue, 3D color-coded signal intensity maps in the 5 transmural shells were obtained representing the scar shape and distribution of the scar tissue (characterized into core and BZ) across the wall thickness (**Figure 1**).

A BZ channel in the ce-CMR reconstruction was defined as a corridor of BZ connecting 2 areas of normal myocardium flowing between 2 core areas or

FIGURE 2 BZ Channel Mass Calculation

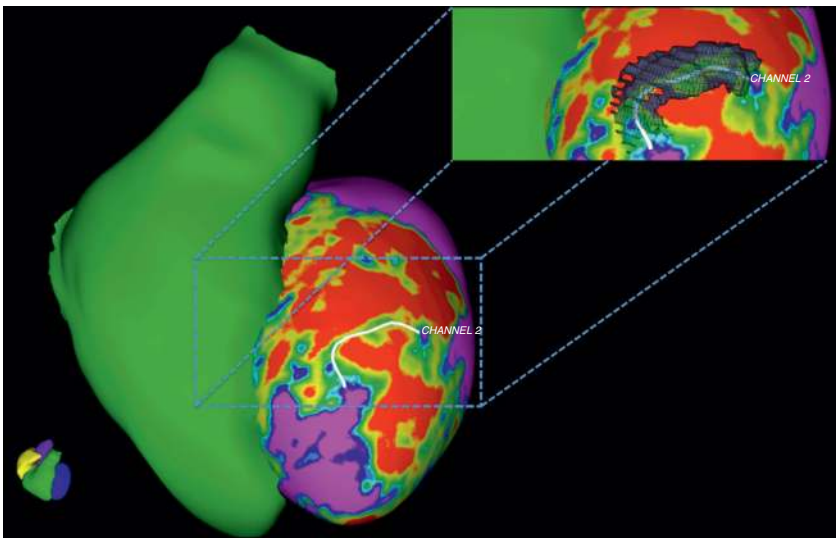

A **white line** is drawn over the surface extending between normal myocardium zones and used as the centerline of a 5-mm radius tube extending beyond the surface **(right)**. This tube enclosed the BZ voxels of the original ce-CMR image that will contribute to the BZ channel mass. BZ = border zone; ce-CMR = contrast-enhanced cardiac magnetic resonance.

TABLE 1 Baseline Characteristics

	All (N = 217)	CRT-D Group (n = 154)	CRT-P Group (n = 63)	p Value*
Age, yrs	65.1 ± 10.5	63.3 ± 10.8	69.5 ± 8.3	<0.001
Male	156 (71.9)	124 (80.5)	32 (50.8)	<0.001
Ischemic cardiomyopathy	86 (39.6)	70 (45.5)	16 (25.4)	0.006
NYHA functional class				0.537
II	77 (35.5)	56 (36.4)	21 (33.3)	
III	130 (59.9)	92 (59.7)	38 (60.3)	
IV	9 (4.1)	5 (3.2)	4 (6.3)	
LVEF, %	26.02 ± 8.04	25.2 ± 7.7	28.08 ± 8.5	0.018
LVESV, ml	242.5 ± 113.8	249.0 ± 109.5	224.2 ± 124.5	0.190
Diabetes	64 (29.5)	43 (27.9)	21 (33.3)	0.621
Atrial fibrillation	40 (18.4)	27 (17.5)	13 (20.6)	0.562
GFR, ml/min	72.2 ± 27.0	75.7 ± 27.5	63.6 ± 23.9	0.005
6MWT, m	297.3 ± 202.3	306.6 ± 137.2	266.9 ± 88.3	0.145
QRS duration, ms	161.7 ± 30.3	161.2 ± 31.6	162.8 ± 27.7	0.747
Medication				
β-blocker	163 (75.1)	117 (75.9)	46 (73.0)	0.707
ACEI/ARB	168 (77.4)	112 (72.7)	44 (69.8)	0.722
Spironolactone	103 (47.5)	71 (46.1)	32 (50.7)	0.875
Diuretic	133 (61.3)	87 (56.4)	46 (73.0)	0.223
Digoxin	32 (14.7)	17 (11.0)	15 (23.0)	0.107
Amiodarone	22 (10.1)	16 (10.3)	6 (9.5)	1.00

Values are mean ± SD or n (%). *CRT-D versus CRT-P groups comparison.

6MWT = 6-min walk test; ACEI = angiotensin-converting enzyme inhibitor; ARB = angiotensin receptor blocker; CRT-D = cardiac resynchronization therapy with defibrillator; CRT-P = cardiac resynchronization therapy with pacemaker; GFR = glomerular filtration rate; LVEF = left ventricular ejection fraction; LVESV = left ventricular end-systolic volume; NYHA = New York Heart Association.

between a core area and a valve annulus (**Figure 2**) (8). An electrophysiologist, blinded to the clinical results, analyzed the 3D reconstructions and identified the BZ channels according to their distribution across the whole LV wall thickness. If the image quality of any set of images was too low to be reconstructed (the presence of artifacts or moderate/severe slice shifting), the set was considered unreadable. Once identified, the BZ channels were manually delineated by drawing a line between areas of normal myocardium. Finally, the BZ channel mass was calculated by multiplying the number of voxels within the BZ channels by voxel mass (**Figure 2**). See the Online Appendix for details.

FOLLOW-UP AND ENDPOINTS. Clinical evaluation was performed before device implantation and every 6 months thereafter. Device interrogation was performed at 1 month after implantation and every 6 months thereafter. The primary endpoint was defined as the composite of appropriate ICD therapy (classified as ATP or shock) or SCD, in order to include all potential life-threatening VAs observed in the study cohort. Inappropriate ICD therapy was recorded. All device interrogations were blinded to ce-CMR results, and all events were reviewed by an event review committee. Echocardiographic and clinical parameters, including LVEF, LV diameters, and New York Heart Association (NYHA) functional class, were

reassessed at 12-month follow-up. Furthermore, total mortality and cardiac mortality were analyzed. The composite of cardiac mortality, SCD, and appropriate ICD therapy was considered as a secondary endpoint.

STATISTICAL ANALYSIS. Continuous data are reported as mean ± SD, and comparisons between groups were performed using the Student *t* test or Mann-Whitney *U* test, as appropriate. Categorical variables are presented as frequencies (percentages) and compared with the chi-square test or Fisher exact method. Receiver-operating characteristic curves were performed to estimate the predictive value of scar variables and to identify cutoff points of interest. For the competing risk analysis, we tabulated the number of patients with each of the 3 outcomes of interest (appropriate ICD therapy, SCD, and death from any other cause). Due to the presence of competing risks, to analyze the effect of baseline predictors on the primary endpoint (appropriate ICD therapy or SCD), we used the cause-specific hazard model for analyzing competing risk survival data as previously described by Austin et al. (10). Variables selected in the univariate analyses ($p < 0.05$) and those considered clinically relevant (LVEF and NYHA functional class, because of its established prognostic value) were entered into multivariate cause-specific hazards models to estimate the independent effect of the scar tissue characteristics on event-free survival for both the primary and secondary endpoints. Scar-related variables were included separately in the multivariate analysis because they were strongly related, and therefore, different multivariate models were needed. Cumulative incidence functions for the primary endpoint and competitive events are provided. For all tests, a p value <0.05 was considered statistically significant. Analysis was performed using SPSS 17.0 software (IBM, Armonk, New York) and R version 3.3.1 (R Foundation for Statistical Computing, Vienna, Austria).

RESULTS

PATIENT POPULATION. Baseline characteristics. A cohort of 235 consecutive patients with class I indication for CRT underwent ce-CMR before device implantation. Eighteen patients (7.6%) were excluded due to low ce-CMR image quality, moderate/severe shifting, or artifacts that prevented appropriate LV segmentation and scar identification. Finally, 217 patients (65.1 ± 10.5 years of age, 71.9% male, 39.6% ischemic) were included in the study. The device implanted was a CRT-D in 154 patients (71%) and a CRT-P in 63 (29%). Baseline clinical characteristics are summarized in Table 1.

TABLE 2 Clinical Characteristics in Patients With Versus Patients Without ICD Therapies/SCD

	ICD Therapy/SCD (n = 25)	No ICD Therapy/SCD (n = 186)	HR (95% CI)	p Value*
Age, yrs	63.2 ± 14.6	65.1 ± 9.9	0.97 (0.94–1.01)	0.09
Male	22 (88.0)	56 (30.1)	3.66 (1.12–12.65)	0.03
Ischemic cardiomyopathy	13 (52.0)	72 (38.7)	1.62 (0.74–3.54)	0.23
NYHA functional class			0.62 (0.41–1.16)	0.24
II	9 (36.0)	67 (36.0)		
III	14 (56.0)	111 (59.7)		
IV	1 (4.0)	8 (4.3)		
Baseline LVEF, %	26.1 ± 8.1	26.2 ± 7.3	0.99 (0.94–1.04)	0.60
12-month LVEF, %	30.6 ± 9.3	36.5 ± 10.9	0.95 (0.89–1.01)	0.131
Baseline LVESV, ml	255.8 ± 108.5	237.5 ± 111.8	1 (0.99–1.01)	0.19
12-month LVESV, ml	166.8 ± 81.0	126.0 ± 84.0	1 (0.99–1.01)	0.605
Diabetes	4 (16.0)	58 (31.2)	0.49 (0.17–1.47)	0.21
Atrial fibrillation	5 (20.0)	34 (18.2)	1.17 (0.44–3.12)	0.75
GFR, ml/min	79.7 ± 33.8	71.3 ± 25.9	1.01 (0.99–1.03)	0.1
QRS duration, ms	163.7 ± 25.9	161.2 ± 31.4	1 (0.99–1.01)	0.93
Medication				
β-Blocker	17 (68.0)	141 (75.8)	0.55 (0.23–1.34)	0.19
ACEI/ARB	16 (64.0)	135 (72.5)	0.62 (0.26–1.45)	0.27
Spironolactone	9 (36.0)	91 (48.9)	0.80 (0.34–1.87)	0.61
Diuretic	15 (60.0)	114 (61.2)	0.61 (0.28–1.44)	0.26
Digoxin	3 (12.0)	28 (15.0)	0.75 (0.22–2.56)	0.653
Amiodarone	1 (4.0)	21 (11.2)	0.41 (0.05–3.04)	0.382

Values are mean ± SD or n (%). Competing risk regression analysis by cause-specific hazard model for the primary endpoint is shown. *ICD Therapy/SCD versus No ICD Therapy/SCD group comparison.

CI = confidence interval; HR = hazard ratio; ICD = implantable cardioverter-defibrillator; other abbreviations as in Table 1.

Follow-up. Six patients (2.7%) were lost to follow-up and were excluded from the analysis. During a median follow-up of 35.5 months (25th to 75th percentiles 12 to 62 months), 25 patients (11.5%) reached the primary endpoint. Five patients (2.3%) died due to SCD; 3 of them had a CRT-P device. Twenty patients (9.2%) received appropriate ICD therapies: 7 received ICD shocks, and 13 were treated with ATP. There were no significant differences in baseline clinical characteristics between patients with or without ICD

TABLE 3 ce-CMR Scar Parameters

	ICD Therapy/SCD (n = 25)	No ICD Therapy/SCD (n = 186)	p Value*
Scar mass, g	38.7 ± 34.2	17.9 ± 17.2	<0.001
BZ mass, g	20.0 ± 22.5	8.7 ± 10.8	<0.001
BZ mass/scar mass ratio	0.49 ± 0.13	0.4 ± 0.21	0.044
Core mass, g	19.0 ± 14.2	9.3 ± 8.7	<0.001
BZ channel mass, g	3.6 ± 3.0	1.8 ± 3.4	<0.001

Values are mean ± SD. *ICD Therapy/SCD versus No ICD Therapy/SCD group comparison.

BZ = border zone; ce-CMR = contrast-enhanced cardiac magnetic resonance; ICD = implantable converter-defibrillator; SCD = sudden cardiac defibrillator.

FIGURE 3 **Homogeneous Scars Without BZ Channels**

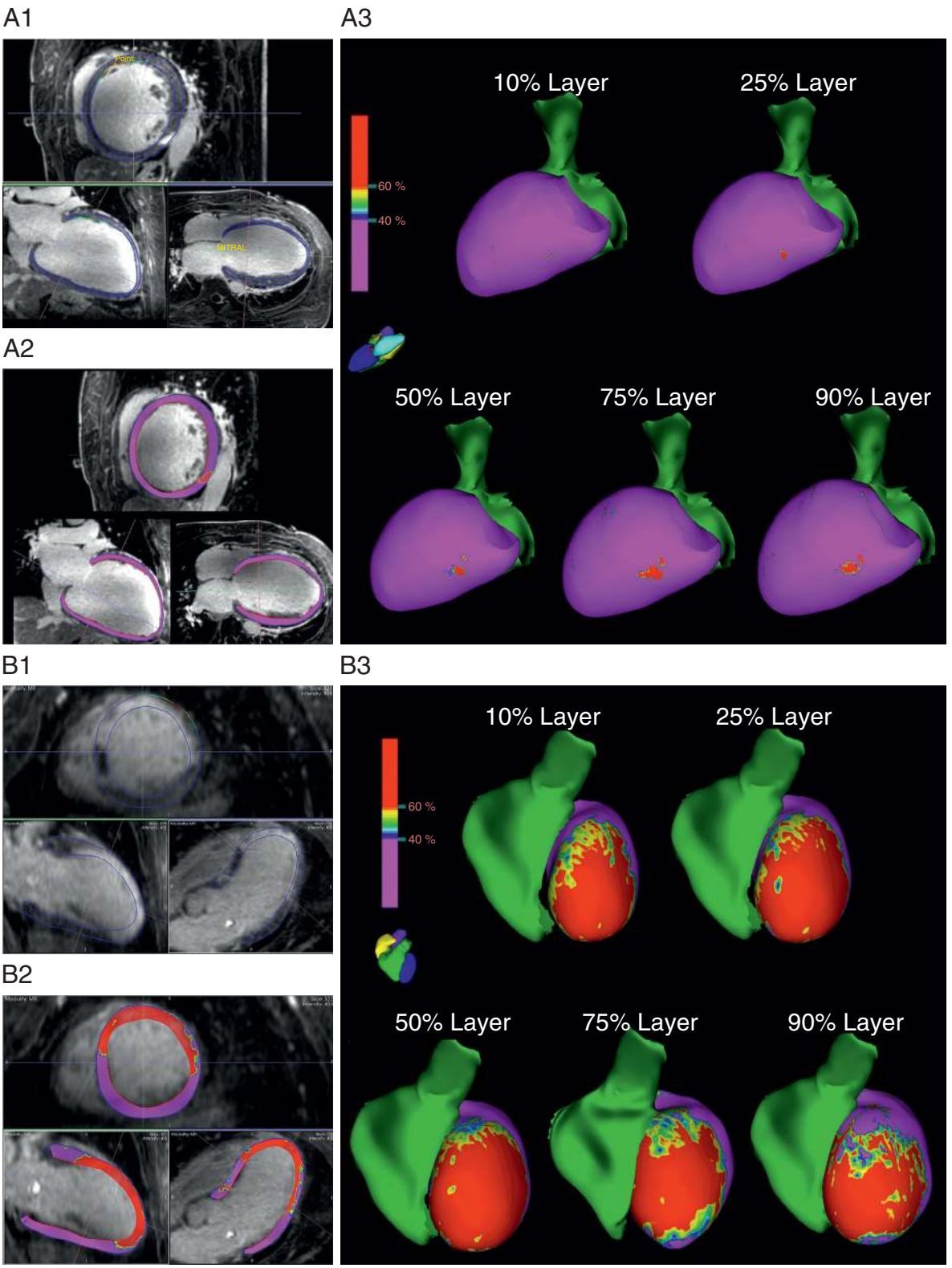

Continued on the next page

therapy/SCD (Table 2). Twelve patients (7.7%) received inappropriate ICD therapies during follow-up: 10 inappropriate shocks (8 due to atrial fibrillation, 1 to electrode noise, 1 to T-wave oversensing) and 2 inappropriate ATP (1 due to atrial fibrillation, 1 to electrode noise). Among patients with CRT-D in whom no therapies were programmed in the fast-VT zone, no episodes of sustained self-limited fast VT were registered.

Mortality. During follow-up, 46 patients (21.1%) died. Cardiac death due to refractory heart failure occurred in 18 patients (39.1%), and SCD occurred in 5 patients (10.8%). Noncardiac death occurred in 18 patients (39.1%), and cause of death could not be determined in 5 patients (10.8%).

ce-CMR ANALYSIS. Late gadolinium enhancement was observed in 125 patients (57.6%). The proportion of patients exhibiting myocardial scar was significantly higher in those assigned to a CRT-D device (66.9% vs. 34.9%; $p < 0.001$).

MYOCARDIAL SCAR SIZE AND CHARACTERISTICS. All patients that reached the primary endpoint during follow-up had myocardial scar; in patients without ICD therapy/SCD, the proportion was 52.1% ($p < 0.001$). None of the patients without myocardial scar experienced ICD therapies or SCD during follow-up. Additionally, in the subgroup of patients with scar ($n = 125$), total scar mass, core mass, and BZ mass were significantly greater in the group with ICD therapies or SCD (Table 3). Furthermore, the scar was not only more extensive, but also more heterogeneous (higher BZ mass/total scar mass ratio) in those patients with ICD therapies or SCD during follow-up (Table 3).

Seventy-four (59.2%) patients with myocardial scar exhibited BZ channels within the scar. BZ channels were observed in all patients with ICD therapies or SCD, compared with less than one-half (49%) of patients without ICD therapies or SCD; $p < 0.001$ (Figure 3). Furthermore, the mass of BZ channels was significantly higher in patients reaching the primary endpoint (3.6 ± 3.0 g vs. 1.8 ± 3.4 g; $p < 0.001$) (Table 3).

PREDICTION OF ARRHYTHMIC EVENTS. The cause-specific hazard model analysis revealed that male sex was the only clinical baseline characteristic associated with ICD therapy or SCD during follow-up (Table 2). On the other hand, all scar parameters were significantly associated with the primary endpoint: scar mass (hazard ratio [HR]: 1.04 [95% confidence interval (CI): 1.03 to 1.05]; $p < 0.001$), core mass (HR: 1.08 [95% CI: 1.05 to 1.1]), BZ mass (HR: 1.06 [95% CI: 1.04 to 1.08]; $p < 0.001$), and BZ channel mass (HR: 1.17 [95% CI: 1.1 to 1.25]; $p < 0.001$).

Three multivariate regression models were created for scar mass (model 1), BZ mass (model 2), and BZ channel mass (model 3) (Table 4). Model 1 was adjusted for LVEF, NYHA functional class, and male sex. In this model, scar mass was the only independent predictor of ICD therapy or SCD (HR: 1.04 [95% CI: 1.03 to 1.05]; $p < 0.001$). Model 2 was adjusted for the same variables, and the only independent predictor was BZ mass (HR: 1.06 [95% CI: 1.04 to 1.08]; $p < 0.001$). Finally, model 3 was adjusted for the same variables, and BZ channel mass was the only independent predictor of the primary endpoint (HR: 1.21 [95% CI: 1.10 to 1.32]; $p < 0.001$).

On the basis of the area under the curve (AUC), scar mass (AUC = 0.891), BZ mass (AUC = 0.897), and BZ channel mass (AUC = 0.894) best predicted the primary endpoint. Scar mass >10 g had 100% sensitivity, 72% specificity, and 30.1% positive predictive value. Scar mass <10 g, present in 134 (61.7%) of patients, had 100% negative predictive value for the occurrence of a primary endpoint.

A BZ mass >5.3 g had 100% sensitivity, 75% specificity, and 32% positive predictive value for the primary endpoint. In 139 patients (64.1%), BZ mass was <5.3 g; this cutoff value had a 100% negative predictive value for the occurrence of ICD therapy or SCD. The cumulative incidence functions showed statistically significant differences in event-free survival for primary endpoint related to scar mass and BZ mass dichotomized by selected cutoff points (Figure 4).

Finally, in order to identify patients at higher risk of reaching the primary endpoint, 2 algorithms were created. A 2-step algorithm based on scar mass >10 g and the presence of BZ channel identified patients reaching the primary endpoint with 100% sensitivity,

FIGURE 3 Continued

None of these patients experienced ICD therapies or SCD during follow-up. **(A)** Short-axis view, 2-chamber view, and 4-chamber view of contrast-enhanced magnetic resonance showing a subepicardial inferolateral focal contrast enhancement **(A1)** and a transmural anterior scar **(B1)**. **(A2/B2)** Concentric layers from the endocardium to epicardium were created and were color-coded according to signal intensity (normal myocardium is in **purple**, border zone in **green**, and core in **red**). **(A3/B3)** 3-Dimensional color-coded signal intensity maps in 5 transmural shells were obtained representing the scar, shape, and distribution of the scar tissue across the wall thickness. BZ = border zone; ICD = implantable cardioverter-defibrillator; SCD = sudden cardiac death.

TABLE 4 Multivariate Competing Risk Regression Analysis for the Association Between Clinical and ce-CMR Parameters and the Study Endpoint of ICD Therapy or SCD

	HR (95% CI)	p Value
Multivariate model 1		
Scar mass, g	1.04 (1.03–1.05)	**<0.001**
Sex	0.70 (0.19–2.63)	0.602
LVEF, %	0.99 (0.93–1.04)	0.621
NYHA functional class I–II vs. III–IV	0.46 (0.19–1.13)	0.241
Multivariate model 2		
BZ mass, g	1.06 (1.04–1.08)	**<0.001**
Sex	0.57 (0.16–2.06)	0.389
LVEF, %	0.98 (0.93–1.04)	0.583
NYHA functional class I–II vs. III–IV	0.51 (0.20–1.28)	0.153
Multivariate model 3		
BZ channel mass, g	1.21 (1.10–1.32)	**<0.001**
Sex	0.42 (0.12–1.51)	0.185
LVEF, %	1.00 (0.95–1.05)	0.977
NYHA functional class I–II vs. III–IV	0.72 (0.30–1.70)	0.455

p Values in bold are significant.
Abbreviations as in Tables 2 and 3.

81.3% specificity, and 36.2% positive predictive value. The second 2-step algorithm, based on scar mass >10 g and BZ mass >5.3 g, predicted the primary endpoint with 100% sensitivity, 79.3% specificity, and 33.3% positive predictive value (Figure 5). Interestingly, the proportion of patients that was classified as low risk by both algorithms was significantly higher in the non-ischemic cohort versus the ischemic group.

MYOCARDIAL SCAR AND SECONDARY ENDPOINT. During follow-up, cardiac death occurred in 23 patients (10.5%): due to refractory heart failure in 18 patients and secondary to SCD in 5 patients. The presence of scar tissue >10 g was an independent predictor of the combined secondary endpoint of cardiac death (due to pump failure or SCD) and ICD therapy (HR: 5.71 [95% CI: 2.86 to 11.38]; $p < 0.001$). Similarly, a BZ mass >5.3 g was independently associated with the secondary endpoint (HR: 4.69 [95% CI: 2.47 to 8.90]; $p < 0.001$).

ISCHEMIC VS. NONISCHEMIC CARDIOMYOPATHY. The univariate analysis revealed no significant association between ischemic cardiomyopathy and the primary endpoint (Table 2). Although areas of delayed enhancement were observed in 90.7% of ischemic patients versus 35.9% of nonischemic patients ($p < 0.001$), it was also the case that among patients with scar, no differences were found in scar mass (23.5 ± 17.4 g vs. 20.6 ± 30.8 g; $p = 0.514$), BZ mass (11.1 ± 11.1 g vs. 11.1 ± 19.1 g; $p = 0.999$), core mass (12.5 ± 9.1 g vs. 9.5 ± 12.8 g; $p = 0.15$), BZ mass/scar mass ratio (0.41 ± 0.19 vs. 0.42 ± 0.21; $p = 0.748$), or BZ channel mass (2.68 ± 3.8 g vs. 1.48 ± 2.7 g; $p = 0.07$) between ischemic and nonischemic patients, respectively.

PREDICTION OF ALL-CAUSE MORTALITY. All-cause mortality was present in 46 patients, of which 23 (50%) died due to cardiovascular causes (heart failure

FIGURE 4 Primary Endpoint Cumulative Incidence

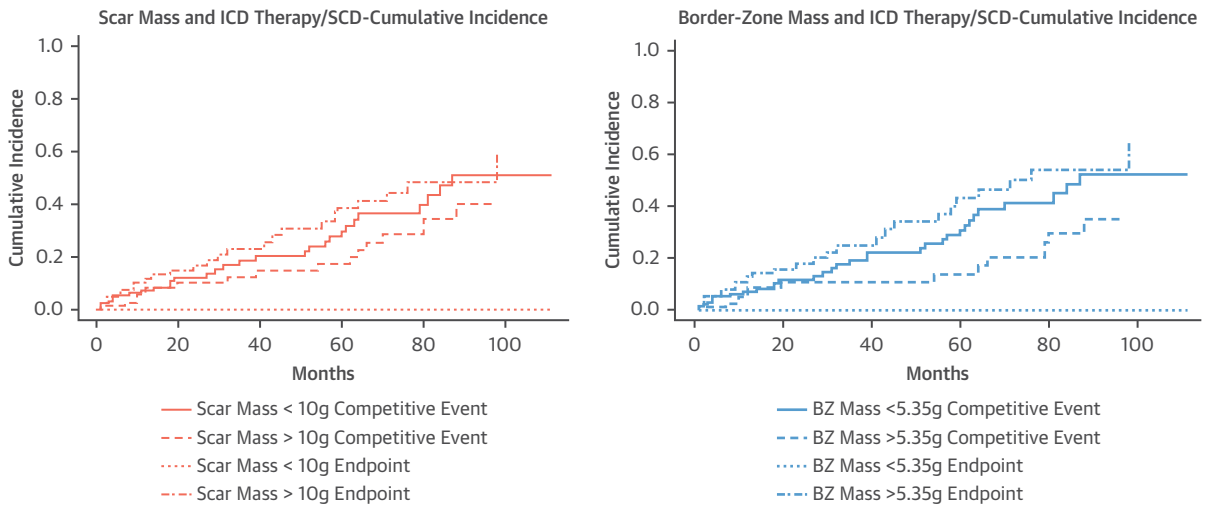

Cumulative incidence functions for primary endpoint and competitive event depending on scar mass **(left)** and border zone mass **(right)**, stratified by optimal cutoff points. Abbreviations as in Figure 3.

FIGURE 5 **Algorithms for ICD Therapies/SCD Risk Stratification in Candidates for CRT**

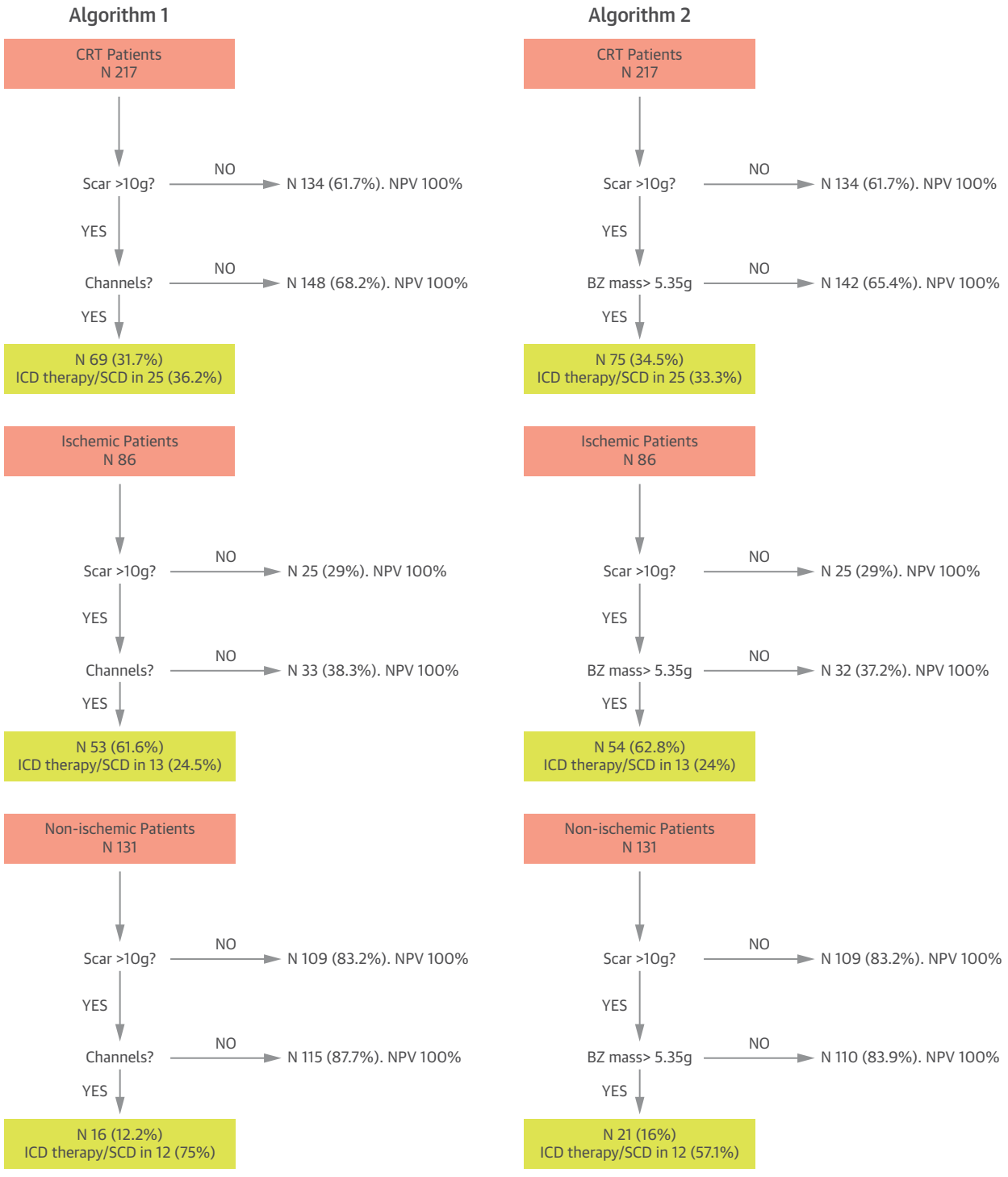

CRT = cardiac resynchronization therapy; NPV = negative predictive value; other abbreviations as in Figure 3.

TABLE 5 Univariate and Multivariate Cox Regression Analysis for the Association Between Clinical and Scar Variables With All-Cause Mortality

	Univariate HR (95% CI)	p Value	Multivariate HR (95% CI)	p Value
Age	1.03 (1.00–1.06)	0.054	1.01 (0.97–1.05)	0.521
Sex	2.05 (1.04–4.02)	0.037	1.57 (0.79–3.32)	0.236
Ischemic cardiomyopathy	1.92 (1.11–3.32)	0.02	1.99 (1.12–3.53)	0.018
NYHA functional class III–IV	2.23 (1.05–4.76)	0.037	2.48 (1.11–5.6)	0.027
LVEF	0.96 (0.92–0.99)	0.028	0.96 (0.93–1.01)	0.09
LVESV	1.00 (0.99–1.01)	0.182		
Diabetes	1.57 (0.88–2.81)	0.123		
Atrial fibrillation	2.04 (1.13–3.7)	0.018	1.80 (0.96–3.35)	0.064
GFR	0.98 (0.97–0.99)	0.001	0.98 (0.97–0.99)	0.016
CRT-D vs. CRT-P	1.11 (0.62–1.98)	0.722		
Scar mass	0.99 (0.98–1.01)	0.84		
Core mass	1.00 (0.98–1.03)	0.829		
BZ mass	0.99 (0.97–1.02)	0.616		
BZ channel mass	0.97 (0.86–1.09)	0.607		

Abbreviations as in Tables 1, 2, and 3.

or sudden cardiac death). None of the scar parameters was significantly associated with all-cause mortality. In multivariate analysis, ischemic cardiomyopathy (HR: 1.99 [95% CI: 1.12 to 3.53]; p = 0.018), NYHA functional class III to IV (HR: 2.48 [95% CI: 1.11 to 5.6]; p = 0.027), and glomerular filtration rate (HR: 0.98 [95% CI: 0.97 to 0.99]; p = 0.016) were independent predictors of all-cause mortality (Table 5).

DISCUSSION

MAIN FINDINGS. The present study analyzed the impact of the presence and characteristics of myocardial scar, assessed by ce-CMR, on the occurrence of appropriate ICD therapies and SCD in PP CRT patients. The main finding was that the extension and heterogeneity of the myocardial scar were independent predictors of ICD therapies/SCD. Specifically, the optimal cutoff value for the scar mass to predict ICD therapies/SCD in the long term was 10 g; no arrhythmic events were observed in patients without scar or with scar mass <10 g. Furthermore, the presence of BZ mass >5.3 g or BZ channels were associated with an additional risk of VA/SCD during follow-up.

CRT-P VS. CRT-D IN PP PATIENTS: RISK STRATIFICATION. No randomized controlled trial to our knowledge has been conducted to date to compare CRT-P versus CRT-D in PP patients. Therefore, the benefit of adding backup ICD capabilities in patients with class I indication for CRT is unknown. In the COMPANION (Comparison of Medical Therapy, Pacing, and Defibrillation in Heart Failure) study, only CRT-D was significantly associated with reduction in SCD (1). However, the study was not designed to compare CRT-D versus CRT-P with the specific endpoint of VA or SCD. On the other hand, long-term results of the CARE-HF (Cardiac Resynchronization-Heart Failure) trial showed a significant 5.6% reduction in SCD risk with CRT-P (11), suggesting that, although the benefit of CRT on heart failure mortality is observed at short-/mid-term, the reduction of SCD risk requires longer follow-up periods.

Given that life-threatening VA has a low incidence in PP CRT patients (1,4), better risk-stratification tools are required. This study showed that the absence of myocardial scar or a scar mass <10 g identified patients at low risk of ICD therapies/SCD during long-term follow-up. Additionally, scar heterogeneity represented an independent predictor of life-threatening arrhythmic events, suggesting the potential utility of scar characterization for risk stratification in CRT patients. In the present study, scar characterization was performed both quantitatively (quantification of BZ mass and BZ mass/scar mass ratio) and qualitatively (identification of BZ channels). Both methods were useful for predicting arrhythmic events. With respect to quantitative analysis, patients reaching the primary endpoint showed more extensive BZ tissue and higher values of BZ mass/scar mass ratio. On the other hand, patients with ICD therapies/SCD also exhibited higher values of BZ constituting BZ channels. In the present study, although the AUC values of BZ mass and BZ channel mass for predicting the primary endpoint were similar, all patients with appropriate ICD therapies or SCD during follow-up showed BZ channels within the scar, suggesting that the BZ distribution creating BZ channels may be more closely related to arrhythmic events than the transitional BZ between core and healthy tissue. Indeed, the algorithm based on scar mass >10 g and the presence of BZ channels identified patients reaching the primary endpoint with a slightly higher specificity (81.3%) than the algorithm based on scar mass >10 g and BZ mass >5.3 g (79.3%) (Figure 5).

Currently, the decision to implant an ICD is primarily based on the presence of severe LV dysfunction. However, in the present study, none of the multivariate models (Table 4) showed LVEF as an independent predictor of ICD therapies or SCD. This is consistent with prior studies reporting that LVEF lacks both sensitivity and specificity in predicting life-threatening arrhythmias (12). On the other hand, the results of the present study highlight the potential of ce-CMR-based scar characterization to improve the specificity of risk stratification by identifying patients with CRT indication (thus, with severe LV dysfunction) at low risk of life-threatening

arrhythmias. This has been corroborated by a recent meta-analysis by Disertori et al. (13) reporting that late gadolinium enhancement was a powerful predictor of ventricular arrhythmias, irrespective of ischemic and nonischemic etiology, especially when LVEF was ≤30%.

Finally, both scar mass >10.0 g and BZ mass >5.3 g, not only predicted the primary endpoint, but also were significantly associated with the secondary combined endpoint of ICD therapy and cardiac mortality. However, none of the scar parameters was associated with all-cause mortality, suggesting that CMR-based tissue characterization could be useful for the prediction of specific cardiac outcomes (cardiac mortality and life-threatening arrhythmias) in CRT patients. The association between scar burden and mortality has been widely studied in ischemic patients. Studies by Kwon et al. (14) and Yan et al. (15) showed that delayed enhancement and scar heterogeneity were powerful predictors of mortality in ischemic patients. On the other hand, Demirel et al. (16) reported that scar characteristics predicted arrhythmic outcomes (sustained VT or ICD therapy) but was not independently associated with all-cause mortality. The present study included both ischemic and nonischemic CRT patients. Furthermore, 50% of deaths were due to noncardiac causes. Although these differences in patients' characteristics and causes of death between this study and previous ones could explain the discrepancies observed in the association between scar characteristics and all-cause mortality, it should be acknowledged that ascertainment of the cause of death is often problematic.

STUDY LIMITATIONS. The main limitation of this study is the low incidence of the primary endpoint, although it was similar to that in larger studies previously published. In 5 patients, 3 of them with a CRT-D device, the cause of death could not be determined; the mean length of follow-up in these patients was 28.4 months (interquartile range: 18 to 39 months), and no arrhythmic event was recorded. Although the mean follow-up period of the present study (35.5 months) is longer than that in the majority of recent studies dealing with the issue of CMR-based risk stratification, the results should be confirmed in larger cohorts with longer follow-up periods. Another potential limitation is the fact that images were acquired either using a 1.5-T or a 3-T clinical scanner, because it remains unknown whether quantitative thresholds of late gadolinium enhancement are interchangeable among different strength scanners. In terms of the study endpoints, programming or not ICD therapies in the fast-VT zone was left to the discretion of the treating physician. However, this programming is consistent with current clinical practice, which makes the results obtained in the present study directly applicable to real-world patients. The primary endpoint was defined as the composite of appropriate ICD therapy (ATP or shock) or SCD, in order to include all potential life-threatening VAs observed in the study cohort. It should be acknowledged that ICD shocks and ATP are not equivalent. Furthermore, there are limitations in using appropriate ICD therapies as a surrogate for SCD. Our definition of primary endpoint is consistent with previous studies on this subject (7,17,18), although it is also the case that other authors did not include ATP as a primary endpoint (12,19,20). It is also possible that self-limited episodes of VT could have been missed in CRT-P patients; however, the clinical relevance of this kind of episode is not well established. Finally, although this was a multicenter study, there is a need for confirmation of these results with a larger patient population and external validation of ce-CMR post-processing method and analysis.

CONCLUSIONS

The presence, extension, heterogeneity, and qualitative distribution of BZ tissue of myocardial scar independently predict appropriate ICD therapies and SCD in CRT patients. Algorithms based on scar mass and BZ distribution or extension correctly identify patients at low risk of life-threatening VAs. These findings warrant future prospective studies for external validation.

ADDRESS FOR CORRESPONDENCE: Dr. Antonio Berruezo, Arrhythmia Section, Cardiology Department, Thorax Institute, Hospital Clinic C/ Villarroel 170, 08036 Barcelona, Spain. E-mail: berruezo@clinic.ub.es.

PERSPECTIVES

COMPETENCY IN MEDICAL KNOWLEDGE: Scar characterization by ce-CMR predicts appropriate ICD therapies and SCD in primary prevention CRT candidates.

TRANSLATIONAL OUTLOOK: A randomized study is required to confirm the usefulness of scar characterization for the identification of CRT candidates that could benefit from adding defibrillator capabilities to the CRT device.

REFERENCES

1. Bristow MR, Saxon LA, Boehmer J, et al. Cardiac-resynchronization therapy with or without an implantable defibrillator in advanced chronic heart failure. N Engl J Med 2004;350:2140–50.

2. Cleland JGF, Daubert J-C, Erdmann E, et al. The effect of cardiac resynchronization on morbidity and mortality in heart failure. N Engl J Med 2005; 352:1539–49.

3. Dickstein K, Vardas PE, Auricchio A, et al. 2010 focused update of ESC guidelines on device therapy in heart failure: an update of the 2008 ESC guidelines for the diagnosis and treatment of acute and chronic heart failure and the 2007 ESC guidelines for cardiac and resynchronization therapy. Eur Heart J 2010;31:2677–87.

4. Moss AJ, Hall WJ, Cannom DS, et al. Cardiac-resynchronization therapy for the prevention of heart-failure events. N Engl J Med 2009;361: 1329–38.

5. Schmidt A, Azevedo CF, Cheng A, et al. Infarct tissue heterogeneity by magnetic resonance imaging identifies enhanced cardiac arrhythmia susceptibility in patients with left ventricular dysfunction. Circulation 2007;115:2006–14.

6. Heidary S, Patel H, Chung J, et al. Quantitative tissue characterization of infarct core and border zone in patients with ischemic cardiomyopathy by magnetic resonance is associated with future cardiovascular events. J Am Coll Cardiol 2010;55: 2762–8.

7. Roes SD, Borleffs CJW, van der Geest RJ, et al. Infarct tissue heterogeneity assessed with contrast-enhanced MRI predicts spontaneous ventricular arrhythmia in patients with ischemic cardiomyopathy and implantable cardioverter-defibrillator. Circ Cardiovasc Imaging 2009;2: 183–90.

8. Fernandez-Armenta J, Berruezo A, Andreu D, et al. Three-dimensional architecture of scar and conducting channels based on high resolution ce-CMR: insights for ventricular tachycardia ablation. Circ Arrhythm Electrophysiol 2013;6:528–37.

9. Andreu D, Ortiz-Perez JT, Fernandez-Armenta J, et al. 3D delayed-enhanced magnetic resonance sequences improve conducting channel delineation prior to ventricular tachycardia ablation. Europace 2015;17:938–45.

10. Austin PC, Lee DS, Fine JP. Introduction to the analysis of survival data in the presence of competing risks. Circulation 2016;133:601–9.

11. Cleland JG, Freemantle N, Erdmann E, et al. Long-term mortality with cardiac resynchronization therapy in the Cardiac Resynchronization-Heart Failure (CARE-HF) trial. Eur J Heart Fail 2012;14:628–34.

12. Klem I, Weinsaft JW, Bahnson TD, et al. Assessment of myocardial scarring improves risk stratification in patients evaluated for cardiac defibrillator implantation. J Am Coll Cardiol 2012; 60:408–20.

13. Disertori M, Rigoni M, Pace N, et al. Myocardial fibrosis assessment by LGE is a powerful predictor of ventricular tachyarrhythmias in ischemic and nonischemic LV dysfunction: a meta-analysis. J Am Coll Cardiol Intv 2016;9:1046–55.

14. Kwon DH, Asamoto L, Popovic ZB, et al. Infarct characterization and quantification by delayed enhancement cardiac magnetic resonance imaging is a powerful independent and incremental predictor of mortality in patients with advanced ischemic cardiomyopathy. Circ Cardiovasc Imaging 2014;7:796–804.

15. Yan AT, Shayne AJ, Brown KA, et al. Characterization of the peri-infarct zone by contrast-enhanced cardiac magnetic resonance imaging is a powerful predictor of post-myocardial infarction mortality. Circulation 2006;114:32–9.

16. Demirel F, Adiyaman A, Timmer JR, et al. Myocardial scar characteristics based on cardiac magnetic resonance imaging is associated with ventricular tachyarrhythmia in patients with ischemic cardiomyopathy. Int J Cardiol 2014;177: 392–9.

17. Boyé P, Abdel-Aty H, Zacharzowsky U, et al. Prediction of life-threatening arrhythmic events in patients with chronic myocardial infarction by contrast-enhanced CMR. J Am Coll Cardiol Img 2011;4:871–9.

18. Scott PA, Morgan JM, Carroll N, et al. The extent of left ventricular scar quantified by late gadolinium enhancement MRI is associated with spontaneous ventricular arrhythmias in patients with coronary artery disease and implantable cardioverter-defibrillators. Circ Arrhythm Electrophysiol 2011;4:324–30.

19. Iles L, Pfluger H, Lefkovits L, et al. Myocardial fibrosis predicts appropriate device therapy in patients with implantable cardioverter-defibrillators for primary prevention of sudden cardiac death. J Am Coll Cardiol 2011; 57:821–8.

20. Wu KC, Gerstenblith G, Guallar E, et al. Combined cardiac magnetic resonance imaging and C-reactive protein levels identify a cohort at low risk for defibrillator firings and death. Circ Cardiovasc Imaging 2012;5:178–86.

KEY WORDS cardiac resynchronization therapy, magnetic resonance imaging, sudden cardiac death, ventricular arrhythmias

APPENDIX For an expanded Methods section, and supplemental figures, please see the online version of this paper.